REFURBISHMENT AND UPGRADE OF FE BOLTZMANN/RAYLEIGH TEMPERATURE LIDAR AT BOULDER FOR A MCMURDO LIDAR CAMPAIGN IN ANTARCTICA

Zhangjun Wang[1, 2], Xinzhao Chu[1], Wentao Huang[1], Weichun Fong[1], John A. Smith[1], and Brendan Roberts[1]

[1] *University of Colorado at Boulder, 216 UCB, CIRES, Boulder, Colorado 80309, USA*
Email: xinzhao.chu@colorado.edu

[2] *Institute of Oceanographic Instrumentation, Shandong Academy of Sciences, Qingdao, Shandong, 266001, China*
Email: zhangjun.wang@hotmail.com

ABSTRACT

For a lidar campaign at McMurdo, Antarctica (77.8°S, 166.7°E) to make year-round measurements of atmospheric temperature, composition, and dynamics with full-diurnal coverage, an alexandrite-laser-based Fe Boltzmann and Rayleigh temperature lidar was upgraded to enhance its specifications via incorporating new technologies. Detailed performance analysis and temperature calibration of the lidar were made at Boulder, Colorado. In this paper we describe the upgrade of the lidar system and present the results of full diurnal measurements made from the Table Mountain Lidar Observatory in Boulder (40°N, 105°W).

1. INTRODUCTION

The mesosphere and lower thermosphere (MLT) is a region of great importance in energy balance processes and a link in vertical energy transfer. The Polar Regions are more sensitive to global change effects than elsewhere and profiles of atmospheric parameters and constituents at the poles can provide a means of validating and calibrating atmospheric models [1]. Despite its unique characteristics, this region remains to this date one of the least explored parts of the Earth atmosphere. The presence of layers that contains metallic atoms and ions such as Na, Fe, K, and Ca opened the field for the resonance fluorescence lidar [2]. Sophisticated observations of middle atmosphere have been made with lidars from the North Pole to South Pole by *Gardner et al.* 2001 [1] and *Chu et al.* 2002 [3].

An Fe Boltzmann lidar developed by Chu, Gardner and co-workers was first deployed on the NSF/NCAR Electra aircraft to make observations of Fe meteor trails during the 1998 Leonid meteor shower [4]. This lidar was then deployed to the North Pole and the Arctic on board the NSF/NCAR Electra aircraft in 1999, to the Amundsen-Scott South Pole Station (90.0°S) from 1999 to 2001, and to Rothera Station (67.5°S) from 2002-2005 [3] for both daytime and nighttime measurements. After working at so many locations with harsh conditions, refurbishment and upgrade of the system was necessary in order to restore its performance. More importantly, incorporating newly available optical and electronic technologies into the existing lidar system will significantly improve its performance and enhance its ability to address the polar observations at McMurdo. These are the subjects of this paper along with test results from Boulder, Colorado.

2. DESCRIPTION OF FE BOLTZMANN TEMPERATURE LIDAR

A schematic of the upgraded lidar system is shown in Fig. 1. The transmitter consists of two lasers operating at 372 and 374 nm, corresponding to resonance lines of the two sublevels of iron atom's ground state. Each transmitter channel consists of an injection-seeded, frequency-doubled, flashlamp-pumped, pulsed alexandrite laser (PAL) and a seed laser. The seed lasers were packaged in a sealed climate chamber that keeps the air temperature and humidity stable. In addition, a Bristol wavelength meter and a scanning Fabry-Perot Interferometer (FPI) are used to control and monitor the seed lasers via a laser-locking program. The output of the seed laser is fiber coupled for injection into the PAL cavity. A dichroic filter was used to separate the fundamental and second harmonic pulses. The outgoing laser beam is expanded by a 6× beam expander to reduce the divergence below 0.35 mrad, and then directed into the sky via a steering mirror. The pulsed output of the alexandrite laser is monitored with a pulsed laser spectrum analyzer and a beam profiler.

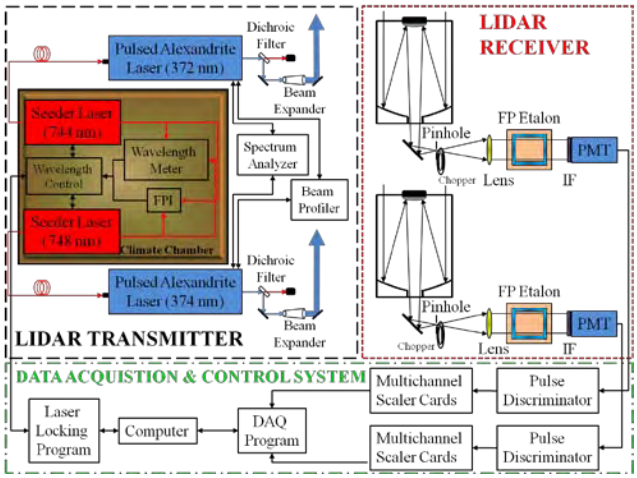

Figure 1. Diagram of the upgraded Fe Boltzmann and Rayleigh temperature lidar system.

Each receiver channel, which is aligned to look in a fixed zenith direction, consists of a 40-cm Schmidt-Cassegrain telescope with enhanced UV dielectric coating. The return signal collected by the telescope is reflected by a 45° high reflection mirror, focused through a field-stop pinhole, collimated by lenses, passes through a daytime etalon filter

and an interference filter, and then detected by a PMT running in photon counting mode. The field of view of the telescope is controlled via the pinhole size at the focal plane and is set to match the divergence of the outgoing laser beam. To prevent PMT saturation by the strong low-altitude returns, a mechanical chopper is placed just behind the field stop in the receiver chain. The output signal from PMT is then thresholded by a discriminator, and the acquisition of two channels' data is handled by the data acquisition system via two multichannel scalers (SR430s).

Unlike the Doppler technique that relies on the temperature dependence of the Doppler broadening of atomic resonance absorption lines, the Boltzmann technique relies on the temperature dependence of the Maxwell–Boltzmann distribution of atomic populations on different atomic energy levels in thermodynamic equilibrium. More detailed information on the operation principle can be found in *Gelbwachs*, 1994 [5] and *Chu et al.*, 2002 [3].

3. LIDAR INSTRUMENT UPGRADE

3.1 Seed laser upgrade

The spectral quality of the output alexandrite laser pulses is largely determined by the spectral purity and optical power of the seed lasers. Degradation of the seed laser quality and power causes alexandrite laser spectrum instability that compromises the lidar performance. We replaced the aged EOSI seed lasers (Model 2010) with two new ECDLs (External Cavity Diode Laser) from Toptica Photonics with higher output power and better stability to improve the stability and spectral purity of the pulsed alexandrite lasers. The injection seed laser is decoupled from the pulse laser by a permanent-magnet Faraday optical isolator. This not only prevents damage to the diode but also ensures untroubled single-mode operation and laser tuning.

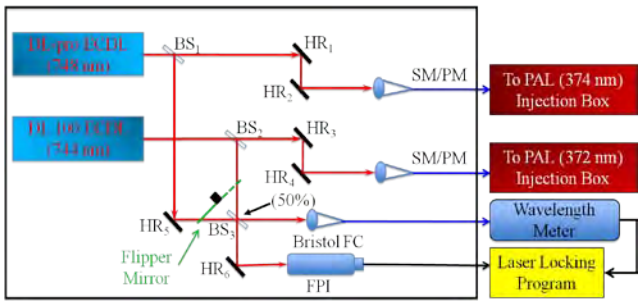

Figure 2. Experimental setup for the injection seeding and wavelength control system.

The experimental setup for the injection seeding and wavelength control system illustrated in Fig. 2, consists of two ECDL seed lasers (Toptica DL 100 and DL- pro), two pulsed alexandrite lasers, a wavelength meter, a scanning FPI, and a laser locking program. The 748 nm laser beam from DL-pro ECDL is split at a beam sampler (BS_1) with 90% power directed by two high reflectivity mirrors (HR_1 and HR_2) and a single-mode polarization-maintained (SM-PM) fiber to the 374 nm PAL. The remaining 10% power is divided by a beam splitter (BS_3) after a high reflectivity mirror (HR_5) with 50% directed through a fiber to the wavelength meter and 50% directed by a high reflectivity mirror (HR_6) to the scanning FPI. The 744 nm seed laser has a setup similar to the 748 nm channel. These two laser systems share the same beam splitter (BS_3) and the mirror HR_6. The flipper mounted with black screen is used to select between the 744 and 748 nm laser beams to be controlled and monitored. That is, the black screen blocks one beam while letting another beam pass through.

In order to reduce the mechanical vibration, all the instruments were fitted on a 24″ by 36″ optical breadboard. The breadboard was packaged in a sealed climate chamber to minimize temperature fluctuations thus helping stabilize the seed laser wavelengths. A new laser-locking program (Section 3.2) was developed to keep the lasers running at the desired wavelengths.

3.2 Lidar Software Upgrade

The software system of the lidar mainly consists of two parts: the data acquisition (DAQ) program and the laser locking program. The initial programs were developed in Window 95® more than a decade ago, so no longer suitable for field deployments. We developed two innovative LabVIEW-based programs by implementing more efficient algorithms and programming with several additional software functionalities.

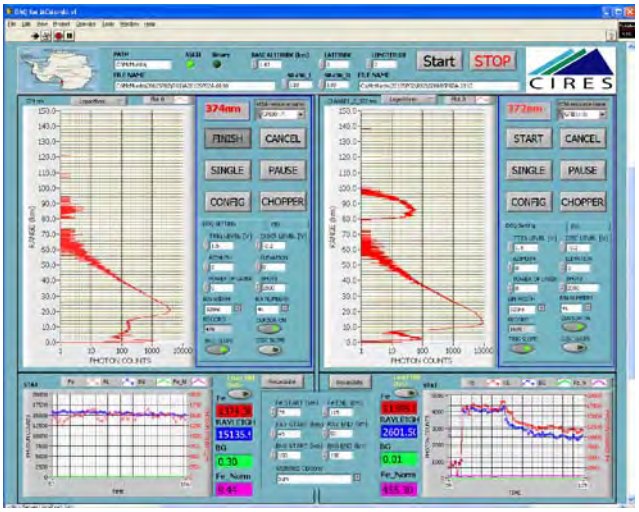

Figure 3. Graphical user interface of the DAQ program. The graph shows the output of the current measurement cycle.

Newly developed DAQ program works with the SR430 device via GPIB card to collect the return photon counts, and then accumulates the signals to certain laser shots before writing the raw profiles into the data storage area. The DAQ User Interface shown in Fig. 3 consists of two main areas and a statistics area.

For each measurement cycle consisting of a number of shots (typically 2000 shots), the range bin counts are accumulated and displayed on-screen. This accumulated pulse count is shown as a function of range, and the display is updated real time. The range is shown on the vertical axis and the photon counts on the horizontal axis. After each measurement cycle, the accumulated photon counts and system parameters are saved in ASCII files. In addition to the data acquisition program, there are several sub-programs responsible for data analysis and data statistics. The range-corrected return-backscatter signal of the Fe lidar is directly related to atmospheric density. For this to be the case full overlap is required between the backscattered laser signal and the field of view of the receive telescope. Time-dependent errors in this alignment compromise the data collection. We did signal statistics to monitor the effects of relative movement of telescope and laser on field overlap. After subtracting the background, we calculate the sum of the signals between 75 and 115 km as the Fe statistics, and the signals between 45 and 50 km as the Rayleigh statistics. When the transmitter and receiver misaligned, the Rayleigh signal level will decrease, providing the operator a good guidance.

The laser locking program is designed specifically for ease of use and flexibility. By calculating the error signal according to the difference between the desired wavelength and the readout of the high-accuracy wavelength meter, the program utilizes the LabVIEW-based PID servo loop to generate a correction voltage. The offset voltage of the PZT is then adjusted according to the external voltage. Then the laser wavelength is locked to the desired wavelength with preset optimized PID parameters. The graphical user interface (GUI) is shown in Fig. 4. It automatically reads and displays the wavelength of 744 nm or 748 nm seed laser in the middle part of the screen. Each seed laser wavelength is sequentially locked according to the setting time when “Flipper Mirror” button is on.

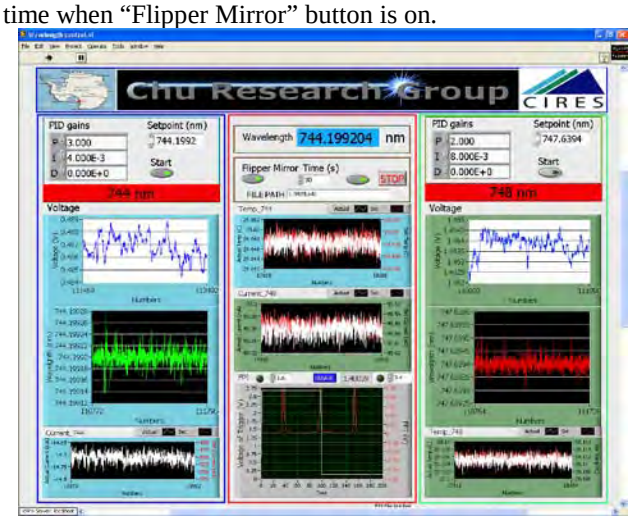

Figure 4. Graphical user interface for the laser wavelength locking program.

The Toptica seed lasers may run into multimodes when the current or temperature has changed too much. So the modes of the seed lasers are sequentially monitored with a scanning confocal FPI (that has a free spectral range (FSR) of 1.5 GHz) and the computer-controlled flipper mirror. The graph in the bottom-middle part of Fig. 4 is used to display the spectrum of the seed laser. All fringes have to be equidistant and should have the same amplitude. In case fringes with different heights occur, changing the diode current can keep the seed laser working in single mode.

The performance of the PID program module can be evaluated from the error signal. The wavelength fluctuation of the stabilized laser is held within ±0.03 pm. In the meantime, there are no frequency drifts and mode hopping, indicating the simple PID program module can run very well for a long time after being activated.

3.3 Daytime Filter Optimization

It would not be acceptable for this lidar to be limited to nighttime since it is deployed in the McMurdo station of Antarctica and the daylight is continuous from November to March. The background of sunlit sky radiance is a significant problem for a lidar operating during daytime.

Considerable care has been taken in the lidar design to minimize the solar background. First, the laser beam is expanded by a beam expander to provide a divergence of less than 350 μrad, which permits the receiver field of view to be limited to approximately 500 μrad. The field of view decreases from 1 mrad to 0.5 mrad by changing the size of pinhole from 4 mm at nighttime to 2 mm at daytime,

Second, narrower spectral bandwidths interference filter are still needed. In order to achieve high solar background suppression, the interference filter was replaced from pass-band width of 5 nm at nighttime to 0.3 nm at daytime.

At last, besides narrowband spectral filtering with a small field of view, the background is reduced with an air-spaced pressure-tuning Fabry-Perot etalon that is temperature and pressure stabilized.

In order to achieve the highest finesse and the narrowest Full-Width-Half-Maximum (FWHM), the etalon is aligned using a Hollow Cathode Lamp (HCL). The etalon is placed into the receiver chain between the interference filter and the collimating lens, and illuminated with the HCL mounted on the top of the telescope. To determine the optimal pressure and alignment of the etalon, the micrometers and the pressure are adjusted until the highest finesse and narrowest FWHM are achieved.

Fig. 5 is a curve of intensity against pressure. The separation of adjacent peaks is the free spectral range of the etalon (650 GHz). The black curve of the peaks at 22.08 psi and 66.5 psi belongs to the 374 nm etalon. The finesse and FWHM of the Etalon are approximately 21 and 30.9 GHz.

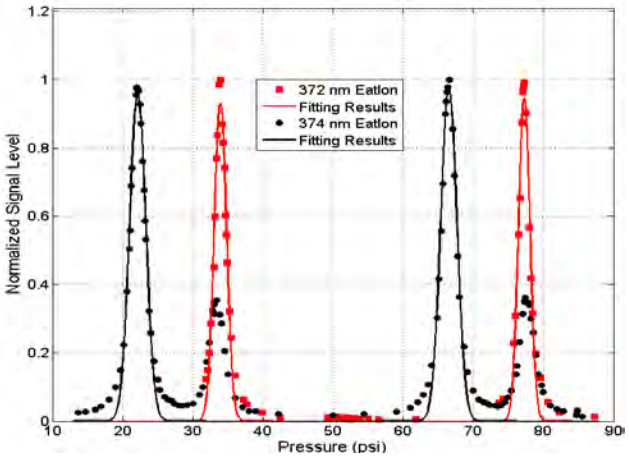

Figure 5. Pressure scans of the 372 nm and 374 nm etalons using a Hollow Cathode Lamp.

4. MEASUREMENT RESULTS

From February to September 2010 the Fe lidar was operated at the Table Mountain Lidar Observatory in Boulder, CO. Figure 6 shows the Rayleigh temperature from 30 km to 75 km with 480 m and 1 hour resolution measured on 5 Sept. 2010, in which the red dash line is the MSIS-90 atmosphere model, and the blue solid line is the experiment data. The difference in Fe temperature between the lidar and MSIS-90 data is plotted on the right .

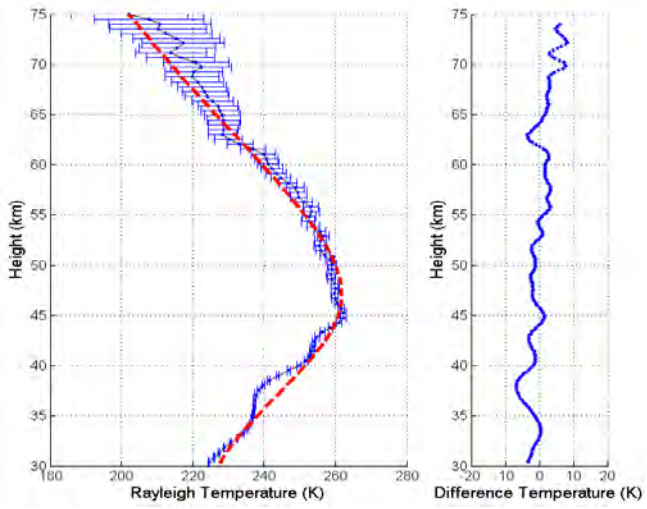

Figure 6. Temperature from 30 km to 75 km measured by this lidar on 05 Sept 2010.

Figure 7 illustrates the 4 days of observations of the Fe temperature in the MLT region and 372 nm Fe density as a function of UT time and altitude at Boulder. Besides the downward phase progression seen in the MLT temperature, an interesting phenomenon is the diurnal variations of the Fe layer, especially at its bottom boundary. The extension of the bottom Fe layer from nighttime to daytime likely reflects the influence of photochemistry on the metal species in the MLT region.

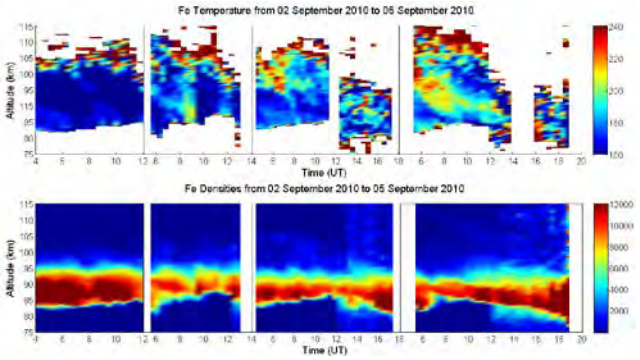

Figure 7. Contour plots of the Fe temperature and Fe layer versus time and altitude from 2-5 Sept 2010 at Boulder. LT = UT – 7.

5. CONCLUSION

A PAL-based Fe Boltzmann temperature lidar has been successfully refurbished and upgraded for measurements of middle and upper atmosphere through the full diurnal cycle. Not only was the lidar performance restored but also greatly enhanced. Newly developed DAQ and seed laser locking program based on LabVIEW makes the lidar much more user friendly. The upgraded Fe Boltzmann temperature lidar has been installed at Arrival Heights, McMurdo in Antarctica in Nov. and Dec. 2010. By now a large amount of lidar data have been collected, revealing many intriguing science discoveries. See a companion paper [6] for details.

ACKNOWLEDGEMENTS

This project was supported by the USA National Science Foundation OPP grant ANT-0839091.

REFERNCES:

1. Gardner, C.S., Papen, G.C., Chu, X., Pan, W., 2001. First lidar observations of middle atmosphere temperatures, Fe densities, and polar mesospheric clouds over the north and south poles. *Geophys. Res. Lett. 28* (7), 1199-1202.

2. Chu, X., and G. C. Papen, Resonance Fluorescence Lidar for Measurements of the Middle and Upper Atmosphere, in the book of *Laser Remote Sensing*, edited by T. Fujii and T. Fukuchi, CRC Press, 2005.

3. Chu, X., Pan, W.L., Papen, G.C., Gardner, C.S., Gelbwachs, J.A., 2002. Fe Boltzmann temperature lidar: design, error analysis, and initial results at the North and South Poles. *Applied Optics 41* (21), 4400-4410.

4. Chu, X., Pan, W., Papen, G.C., Gardner, C.S., Swenson, G., Jenniskens, P., 2000. Characteristics of Fe ablation trails observed during the 1998 Leonid meteor shower. *Geophys. Res. Lett. 27*, 1807-1810.

5. Gelbwachs, J.A., 1994. Iron Boltzmann factor LIDAR: proposed new remote-sensing technique for mesospheric temperature. Applied Optics 33, 7151-7156.

6. Chu, X., et al., McMurdo lidar campaign: A new look into polar upper atmosphere, *Proc. 26th ILRC*, Greece, June 2012.